

Attrition resistance of spray-dried iron F–T catalysts: effect of activation conditions

Rong Zhao^a, Kandis Sudsakorn^a, James G. Goodwin Jr.^{b,*},
K. Jothimurugesan^c, Santosh K. Gangwal^d, James J. Spivey^e

^a Department of Chemical and Petroleum Engineering, University of Pittsburgh, Pittsburgh, PA 15261, USA

^b Department of Chemical Engineering, Clemson University, Clemson, SC 29634, USA

^c Department of Chemical Engineering, Hampton University, Hampton, VA 23668, USA

^d Research Triangle Institute, P.O. Box 12194, Research Triangle Park, NC 27709, USA

^e Department of Chemical Engineering, North Carolina State University, Raleigh, NC 27695, USA

Abstract

The focus of the research reported herein was to investigate the effects of phase changes, as occur during Fe catalyst activation and Fischer–Tropsch synthesis, on Fe catalyst attrition resistance. Different activation conditions (CO, H₂ or syngas) were applied prior to attrition testing to a selected spray-dried Fe catalyst containing 9.1 wt.% binder SiO₂, which had been shown to have the highest attrition resistance in our early study of calcined catalysts. Although, XRD indicated that different Fe phase compositions resulted in the differently activated catalyst samples, chemical attrition was not observed for any of the samples. The BET surface areas of the activated samples were smaller than that of the calcined precursor but no significant changes in pore volume and particle size were found. The attrition resistances of the differently activated catalyst samples were found to be similar to that of the calcined catalyst for this spray-dried Fe catalyst. Attrition resistance was found previously to be governed by catalyst particle density, which has been shown earlier to relate to the SiO₂ network in catalysts. It is therefore suggested that the type and concentration of SiO₂ that is incorporated during the preparation of spray-dried Fe catalysts have a much more significant impact on catalyst attrition than Fe phase change during activation in the presence of CO, H₂ or H₂ + CO. © 2002 Elsevier Science B.V. All rights reserved.

Keywords: Attrition resistance; Fischer–Tropsch synthesis; Activation conditions; BET surface area; Spray-dried Fe catalysts

1. Introduction

Due to their excellent water-gas shift (WGS) capability, iron (Fe) catalysts are the preferred catalysts for Fischer–Tropsch synthesis (FTS) based on coal [1,2]. However, catalyst attrition, causing plugging of downstream filters and product contamination, is one of the major problems encountered in the industrial

application of Fe Fischer–Tropsch (F–T) catalysts in slurry bubble column reactors (SBCRs) [3], the preferred type of reactor for this highly exothermic reaction. In order to improve the attrition resistance of Fe catalysts without sacrificing their activities and selectivities, spray drying has been employed in the preparation of a new generation of Fe F–T catalysts with improved physical strength [4–7].

In our previous studies, spray drying in combination with catalyst composition was used and found to improve significantly the catalyst attrition resistance [8,9]. In a study of the catalysts in their calcined form

* Corresponding author. Tel.: +1-864-656-6055;

fax: +1-864-656-0784.

E-mail address: jgoodwi@clemson.edu (J.G. Goodwin Jr.).

[8], it was found that catalyst particle density is one of the most critical particle properties that affect the final attrition performance. The SiO_2 incorporated in these spray-dried catalysts was found to be evenly distributed throughout the catalyst particles. The SiO_2 structure in the catalyst particles, however, was found to be dependent on SiO_2 type and concentration and was suggested to determine catalyst particle density as well as its attrition resistance. After carburization by CO [9], the majority component of the catalysts (Fe) was carburized to Fe carbides, mostly χ -carbide (Fe_5C_2). Significant decreases, in general, in average catalyst particle size and BET surface area were also observed. For catalysts with lower concentrations of SiO_2 , chemical attrition was observed resulting in the breakage of individual catalyst particles and the formation of sub-micrometer scale fines. Such chemical attrition appeared to be eliminated to a significant degree with an increase in the SiO_2 concentration. Only a break up of large particle agglomerates was observed for catalysts with higher SiO_2 concentrations and the catalyst particles remained spherical after carburization. SiO_2 type (binder vs. precipitated SiO_2) and concentration were suggested to remain the critical parameters that determine the attrition performance of these catalysts in the carburized form despite the phase change in Fe.

Even though we have found comparable attrition resistances for the carburized catalysts as for the same catalysts in their calcined form, it is still of concern that different activation conditions, which result in different Fe phase compositions, might have an effect on catalyst attrition, especially during the initial stage of reaction. The effect of pretreatment on catalyst activities and selectivities has been studied intensively [10–12]. H_2 , CO or syngas ($\text{CO} + \text{H}_2$) has been typically used in Fe catalyst activation and it has been found that catalyst activity and selectivity can differ at initial and steady-state stages as a result of differences in activation conditions [12,13]. Although it has been shown that, for spray-dried Fe catalysts having moderate SiO_2 concentrations, conversion of hematite (Fe_2O_3) to χ -carbide does not appear to cause much chemical attrition except the break up of large agglomerates [9], it is still of interest to find out the effect of Fe phase change to magnetite (Fe_3O_4) and other carbides. In addition, any effect of water vapor formation (when H_2 or syngas ($\text{CO} + \text{H}_2$) activation is used)

and/or higher hydrocarbon formation in the catalyst pores (when syngas activation is used) on catalyst attrition resistance is still not clear.

This study focused on developing a better understanding of the effect of different activation conditions on Fe catalyst attrition, both physical and chemical.

2. Experimental

2.1. Catalyst

A spray-dried, Cu- and K-promoted Fe catalyst was used in this study. Binder SiO_2 of ca. 9.1 wt.% of the total catalyst weight was incorporated during catalyst preparation. The catalyst was spray-dried at 250°C in a Niro spray drier and was then calcined at 300°C for 5 h in a muffle furnace. The detailed catalyst preparation conditions and procedures have been described previously [6,7]. After calcination, the catalyst was sieved between 38 and $90\ \mu\text{m}$ prior to activation. It was not sieved again after the activation procedures. This catalyst had been determined to have superior attrition resistance (comparable to $\text{Co}/\text{Al}_2\text{O}_3$) in both its calcined and carburized (Fe_5C_2) forms in our previous studies [8,9] and was therefore chosen for this study. The activity and selectivity of this catalyst has been determined using a fixed-bed reactor and was found to be comparable to the Ruhrchemie Fe F–T catalyst [6,7].

2.2. Catalyst activation

Catalyst activation was conducted in a quartz fixed-bed reactor. For each experiment, 7 g of catalyst was loaded into the reactor prior to activation. The pretreatments were conducted under H_2 , CO or syngas ($\text{CO} + \text{H}_2$), respectively. The catalyst was heated under atmospheric pressure from room temperature to 280°C at a ramping rate of approximately $1^\circ\text{C}/\text{min}$ and kept at 280°C for 12 h. The detailed pretreatment conditions for each activation are summarized in Table 1. After each pretreatment was completed, the catalyst was cooled down to room temperature under helium with a flow rate of about $50\ \text{cm}^3/\text{min}$. When room temperature was reached, the passivation of the activated catalyst was carried out using a 5% O_2 in helium flow which was first at $20\ \text{cm}^3/\text{min}$ and then gradually increased to $50\ \text{cm}^3/\text{min}$. An

Table 1
Activation conditions^a and nomenclature

Pretreatment	Pretreatment gas	Flow rate (cm ³ /min)
Calcination	No activation applied	
H ₂ activation	H ₂	350
Syngas activation	H ₂ /CO = 2/3	375 ^b
CO activation (LF) ^c	CO	185
CO activation (HF) ^d	CO	375

^a Activation conditions: $T = 280^{\circ}\text{C}$, ramping rate: $1^{\circ}\text{C}/\text{min}$, TOS at 280°C for 12 h, $P_{\text{T}} = 1 \text{ atm}$.

^b Total flow rate of CO and H₂.

^c Low flow rate.

^d High flow rate.

increase in temperature in the catalyst bed of ca. $5\text{--}15^{\circ}\text{C}$ was observed after the start of the passivation but the temperature returned to ambient by the end of passivation. After room temperature was reached, the catalyst was carefully removed from the reactor and stored in a sealed container. Such a passivation procedure has been suggested to result in a thin layer (no more than 1–2 nm) of Fe oxide on the surface of the catalyst particles that preserves the bulk of the catalysts particles from further oxidation [14].

2.3. Catalyst characterization

Catalyst attrition testing was performed in a jet cup system as described previously [15,16] except that N₂ flow was used instead of air in order to avoid further oxidation of the catalysts during attrition testing. For all the attrition measurements, a 15 l/min N₂ flow at atmospheric pressure was employed having a relative humidity of $60 \pm 5\%$. After 1 h time-on-stream (TOS), the N₂ flow was stopped and the weight of fines collected by the downstream filter was determined and “weight percentage of fines lost” calculated.

Powder XRD patterns of the catalyst samples after pretreatment was determined on a Philips X’pert Diffractometer. Catalyst BET surface areas and pore volumes were measured using a Micromeritics automated system. All catalyst samples were degassed before BET surface area and pore volume measurements. The degassing was carried out under vacuum at 100°C for 1 h and then 300°C for 3 h for each sample. It is believed that most, if not all, of the higher hydrocarbons that deposited in the pores of

the syngas-activated catalyst were removed under such degassing conditions; however, carbonaceous deposits (such as coke) would not have been removed. Catalyst particle size distributions before and after attrition testing were measured using a Microtrac laser particle size analyzer. SEM measurements were used to obtain the catalyst morphology. Mercury intrusion was carried out to determine particle density (particle mass divided by its volume) and skeletal density (particle mass divided by its volume excluding all open pores). However, as reported previously [8], particle density rather than skeletal density has been found to govern attrition of spray-dried Fe catalysts and, hence, it was measured here. Detailed descriptions of sample characterization and handling procedure can be found in our previous papers [8,9,15,16].

3. Results

3.1. Catalyst phase composition

Phase compositions of the catalyst before and after activation were determined using XRD and are summarized in Table 2. The major crystalline constituent of the calcined catalyst was hematite, Fe₂O₃. After activation under different conditions, hematite in the catalyst was reduced and/or carburized to different degrees and the resulting catalyst consisted of different Fe phases. It has been suggested [17] that hematite is first reduced to magnetite (Fe₃O₄) under H₂, CO or syngas. Depending on the activation and reaction conditions, magnetite can be further reduced to $\alpha\text{-Fe}$ or carburized to various carbides. Therefore, Fe phase composition in the catalyst is highly dependent on gas phase composition, TOS, temperature, pressure and space velocity of the pretreatment gas. As shown in Table 2, during H₂ activation, the catalyst was partially reduced to $\alpha\text{-Fe}$ and magnetite. CO activation was found to reduce the catalyst initially to mostly magnetite, as shown in the activation procedure using a lower space velocity of CO (LF). With the increase in CO flow rate during the same TOS (HF), the catalyst was further carburized to mainly χ -carbide (Fe₅C₂). Syngas-activated catalyst consisted mainly of magnetite and ϵ' -carbide. These results are similar to those that have been reported before [18,19].

Table 2
Characteristics of the pretreated catalyst before attrition testing

Pretreatment	Phase composition	Average particle size (mm) ^a	BET surface area (m ² /g) ^a	Pore volume (cm ³ /g) ^b	Particle density (g/cm ³) ^a
Calcination	Fe ₂ O ₃	75	95	0.26	2.42 ^c
H ₂ activation	Fe ₃ O ₄ + α -Fe	73	69	0.27	2.01
Syngas activation	Fe ₃ O ₄ + Fe _{2.2} C	71	60	0.21	1.98
CO activation (LF)	Fe ₃ O ₄	75	86	0.25	1.88
CO activation (HF)	Fe ₅ C ₂	73	62	0.24	1.54

^a Error: $\pm 5\%$ of the value measured.

^b Error: $\pm 10\%$ of the value measured.

^c Average of three measurements.

3.2. Particle size, porosity and density

Besides phase composition, other particle properties were also determined for the calcined and activated catalyst prior to physical attrition testing. The results are also summarized in Table 2.

It can be seen that the average particle size of the catalyst remained almost unchanged within experimental error. It has been reported that carburization can cause a decrease in catalyst particle size [9]. However, the degree of decrease in particle size for a spray-dried Fe catalyst is dependent on catalyst composition and inner particle structure [9]. The decrease in catalyst particle size for this catalyst was within the experimental error of the particle size distribution measurement.

The BET surface areas of the activated samples were obviously smaller compared to the calcined catalyst. But the pore volume was found essentially unchanged after activation. In a previous study [12], both BET surface area and pore volume of an activated Fe catalyst were found to be smaller compared to the calcined catalyst. In our previous study [9] of carburized Fe catalysts, it was also found that the pore volume decreased during carburization. However, it is suggested that the degree of the decrease in pore volume is also dependent on catalyst composition. Hence, based on experimental results, the change in pore volume was small and negligible for this particular catalyst. Since, all the activated catalysts were degassed before BET surface measurement, any hydrocarbons that deposited in the catalyst pores during syngas activation can be considered to be essentially fully removed. Therefore, the decreases in BET surface area and pore volume

for the syngas-activated catalyst were probably not caused by any plugging of catalyst pores by hydrocarbon products but may have been caused in part by coke deposition.

The particle densities of all the catalyst samples activated differently were rather close to each other. However, decreasing particle density can be observed as a result of formation of Fe₃O₄, Fe and Fe carbide (Table 2).

3.3. Catalyst morphology

The catalyst samples after activation were investigated using SEM for any possible chemical attrition. The morphology of the calcined catalyst (Fig. 1) can be compared to that of the activated samples (Figs. 2 and 3). The SEM micrographs confirm the results of particle size distribution measurement which showed that particle size was almost unchanged after the various activation procedures. Most of the particle agglomerates remained after activation and there was no observed breakage of the individual particles. For the catalyst activated under syngas (Fig. 2(D)), it can be seen that break up of particle agglomerates and decrease in average catalyst particle size were more obvious than for the other activated samples (Fig. 2(A)–(C)).

At higher magnification, as seen in Fig. 3, there were slight differences in the surface morphologies of the differently activated catalyst samples. But all of the catalyst samples after activation exhibited relatively smooth surfaces with no obvious flaws or cracks. Also, for all the samples after activation, no fines formation was observed.

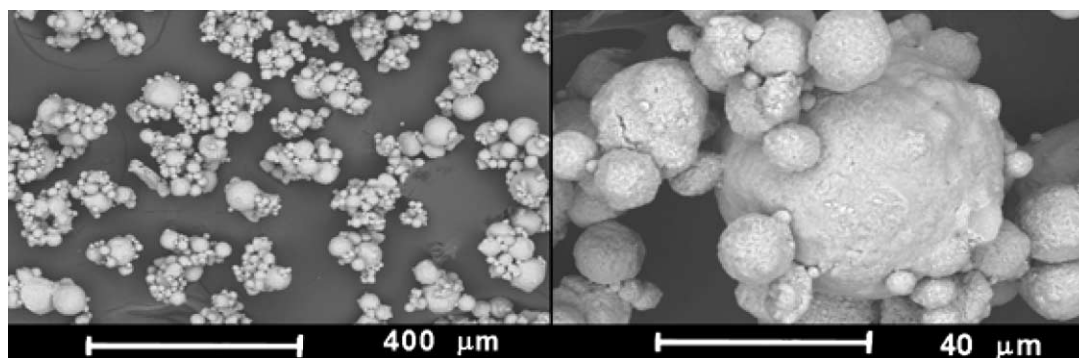


Fig. 1. Morphology of the calcined catalyst.

3.4. Catalyst attrition

Catalyst attrition as determined by jet cup measurement is given in Table 3. All the activated samples appeared to attrit to a similar degree as indicated by both the attrition indices, net change in volume moment (where the volume moment is a measure of aver-

age particle size) and weight percentage of fines lost. Table 3 clearly shows that the calcined catalyst generated the lowest % fines lost and that the % fines lost increased with the inclusion of CO in the pretreatment gas. This is consistent with the density results in Table 2 where the samples with higher densities had higher attrition resistances and generated less fines.

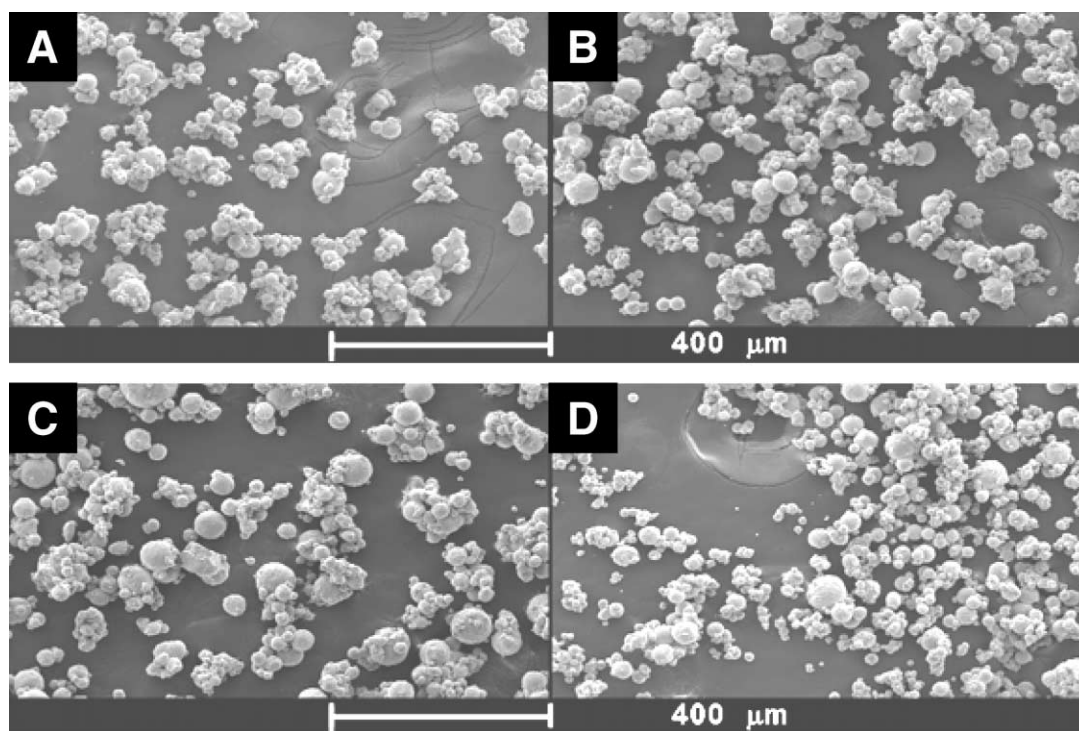


Fig. 2. Morphology of the activated samples at low magnification: (A) H₂-activated catalyst; (B) CO (lower flow rate)-activated catalyst; (C) CO (higher flow rate)-activated catalyst; (D) syngas (CO + H₂)-activated catalyst.

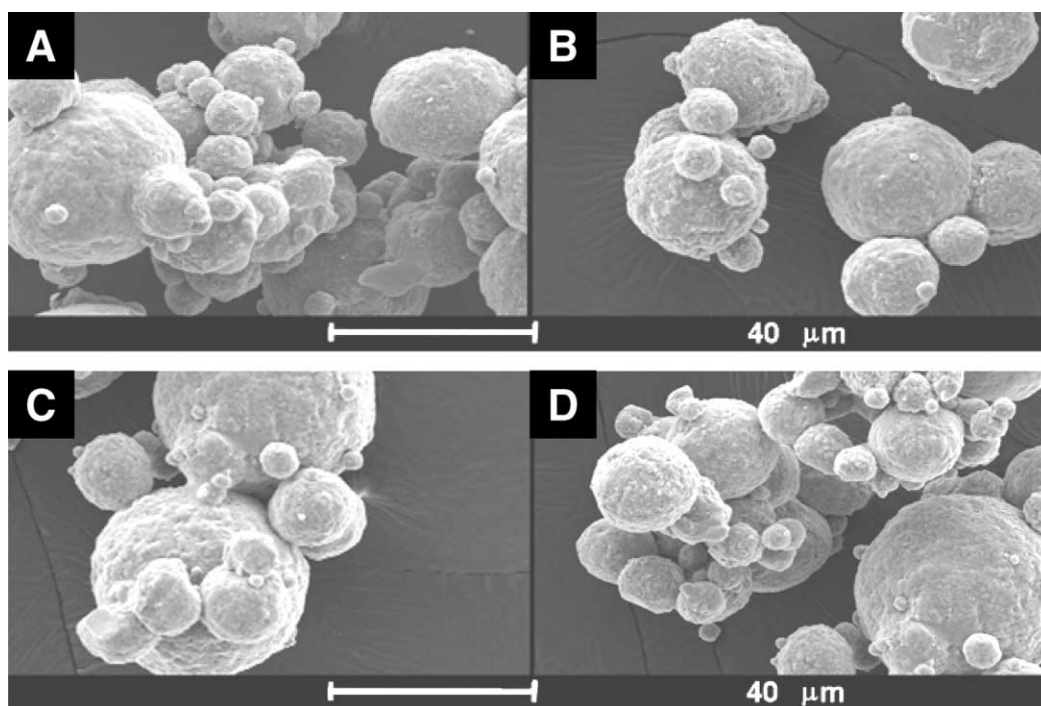


Fig. 3. Morphology of the activated samples at high magnification: (A) H₂-activated catalyst; (B) CO (lower flow rate)-activated catalyst; (C) CO (higher flow rate)-activated catalyst; (D) syngas (CO + H₂)-activated catalyst.

Table 3

Jet cup attrition test results of the spray-dried iron catalysts before and after activation

Catalyst	Net change in volume moment (%) ^{a,b,c}	Fines lost (wt.%) ^{d,e}
Calcined catalyst	24.0	4.4
H ₂ activation	23.2	4.7
Syngas activation	25.9	5.6
CO activation (LF)	31.9	7.5
CO activation (HF)	29.8	7.7
Co/Zr/SiO ₂ ^f	43.5	31.07
Co/Ru/Al ₂ O ₃ ^g	15.2	6.2

^a Net change in volume moment was determined with reference to the particle size distribution before attrition testing.

^b Net change in volume moment (VM) = [(VM of sample after attrition test – VM of sample before test)/VM of sample before test] × 100%.

^c Error: ±5% of the value measured.

^d Weight percentage of fines = weight of fines collected/weight of total catalyst recovered × 100%.

^e Error: ±10% of the value measured.

^f Co/Zr/SiO₂ was a Davison 952 silica-supported 20 wt.% cobalt catalyst.

^g Co/Ru/Al₂O₃ was a Vista B alumina-supported 20 wt.% cobalt catalyst.

4. Discussion

4.1. Chemical attrition

SEM provides an easy evaluation of any possible chemical attrition. As shown in our previous study [9], chemical attrition can result in breakage of individual particles, formation of sub-micrometer scale fines, and break up of large particle agglomerates for many of the Fe catalysts we have studied. Breakage of individual particles and formation of fines can be harmful during SBCR operation since, it can cause filter plugging problems and product contamination. However, break up of large particle agglomerates is a less serious problem in terms of SBCR operation, especially when the resulting primary spherical catalyst particles are large enough and have sufficient physical strength.

For all the activated samples of this spray-dried Fe catalyst (containing 9.1 wt.% binder SiO₂) studied, chemical attrition was found to be negligible. There were no fines formation or breakage of individual primary particles observed for the catalyst samples

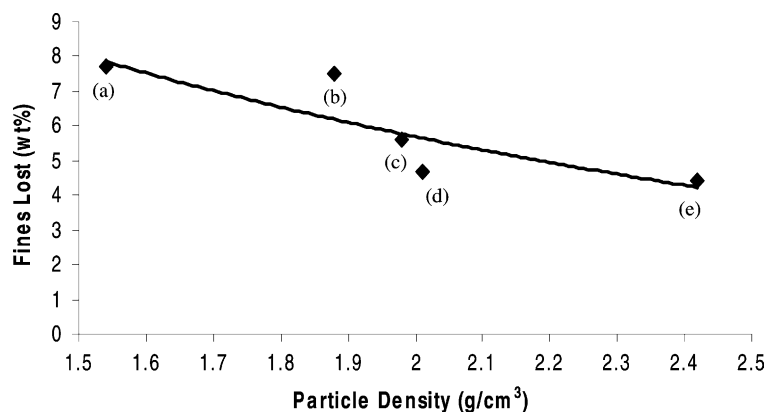


Fig. 4. Fines lost vs. particle density: (a) calcined; (b) H₂ activation; (c) syngas activation; (d) CO activation (LF); (e) CO activation (HF).

activated differently (Fig. 3). Break up of agglomerates was observed but not found to be severe (Fig. 2). Even in the presence of water vapor with (during H₂ + CO treatment) or without (during H₂ treatment) the formation of higher hydrocarbons, it was found that breakage of the catalyst particles did not occur. Since, it has been found that Fe phase change can cause chemical attrition of spray-dried Fe catalysts having low SiO₂ concentrations, it is suggested that chemical attrition did not occur for the catalyst studied due to the presence of a SiO₂ network in the particle structure.

4.2. Physical attrition

Fe phase change, in addition to causing chemical attrition, can cause changes in catalyst particle structure. Change in particle inner structure can have an impact on catalyst physical strength and on catalyst particle density. Particle density also has an effect on catalyst physical strength. Thus, it is not surprising that both catalyst particle structure and particle density have been found to influence the attrition resistance of spray-dried Fe catalysts [8,9]. Furthermore, particle density is one of the parameters that affect directly to fluidization of catalyst particles in jet cup. However, it has been shown earlier [8,9] that attrition properties of Fe catalysts in the jet cup depend only slightly on fluidization but strongly on particle density. Here, the plot of the attrition index (% fines lost) against particle density of the differently activated catalysts, Fig. 4, shows clearly a similar pattern of dependence of

catalyst attrition on particle density. A similar result was also found for the other attrition index-net change in volume moment.

Under different activation conditions, this Fe catalyst has been shown to go through extensive phase changes. However, none of the phase changes appeared to affect chemical or physical catalyst attrition. The formation of water vapor and hydrocarbons did not appear to greatly change catalyst physical attrition resistance either. Comparing these results to those for several supported Co catalysts (Table 3) that have been successfully tested using a laboratory SBCR [15], it appears that this Fe catalyst, before and after activation, has sufficient attrition resistance for extended use in SBCRs. It can be suggested that catalyst composition, especially SiO₂ type and concentration, is the dominant factor that determines the attrition resistance of spray-dried Fe catalysts.

5. Conclusion

Fe phase changes, which have been reported during Fe catalyst activation, would be expected to affect the attrition resistance of Fe F–T catalysts. In addition to Fe phase change, any water vapor and higher hydrocarbon formation during H₂ reduction or syngas pretreatment might also have an effect on catalyst attrition resistance. Recently, we have reported the preparation of an attrition-resistant spray-dried Fe F–T catalyst family. In our present study, the optimum

attrition-resistant spray-dried Fe F–T catalyst of this series containing 9.1 wt.% of binder SiO_2 was used to study the impact of catalyst activation on attrition resistance. The physical strengths of the differently activated catalyst samples were found to be close to that of the calcined catalyst. No chemical attrition was observed for any of the differently activated samples except for the breakup of some large particle agglomerates. It is suggested that the dominant parameters that affect catalyst attrition resistance in spray-dried Fe F–T catalysts is the type (binder vs. precipitated) and concentration of SiO_2 incorporated during preparation.

Acknowledgements

Financial support by the Department of Energy (Office of Fossil Energy) under Grant No. DE-FG22-96PC96217 is gratefully acknowledged.

References

- [1] M.E. Dry, in: J.R. Anderson, M. Boudart (Eds.), *Catalysis—Science and Technology*, Vol. 1, Springer, New York, 1981, p. 160 (Chapter 4).
- [2] R.B. Anderson, *The Fischer–Tropsch Synthesis*, Academic Press, New York, 1984.
- [3] C.-S. Huang, L. Xu, B.H. Davis, *Fuel Sci. Technol. Int.* 11 (1993) 639.
- [4] H. Pham, A.K. Datye, *Catal. Today* 58 (2000) 233.
- [5] D.B. Bukur, L. Nowicki, S.A. Patel, *Can. J. Chem. Eng.* 74 (1996) 399.
- [6] K. Jothimurugesan, J.G. Goodwin Jr., J.J. Spivey, S.K. Gangwal, in: *Proceedings of the 217th ACS National Meeting, Symposium on Syngas Conversion to Fuels and Chemicals*, American Chemical Society, Anaheim, CA, March 21–25, 1999.
- [7] K. Jothimurugesan, J.G. Goodwin Jr., S.K. Santosh, J.J. Spivey, *Catal. Today* 58 (2000) 335.
- [8] R. Zhao, J.G. Goodwin Jr., K. Jothimurugesan, J.J. Spivey, S.K. Gangwal, *Ind. Eng. Chem. Res. IE&CR* 40 (2001) 1065.
- [9] R. Zhao, J.G. Goodwin Jr., K. Jothimurugesan, J.J. Spivey, S.K. Gangwal, *Ind. Eng. Chem. Res. IE&CR* 40 (2001) 1320.
- [10] R.B. Anderson, in: P.H. Emmett (Ed.), *Hydrocarbon Synthesis, Hydrogenation and Cyclization*, Reinhold, New York, 1956.
- [11] D.B. Bukur, L. Nowicki, R.K. Manne, X. Lang, *J. Catal.* 155 (1995) 366.
- [12] D.B. Bukur, X. Lang, Y. Ding, *Appl. Catal. A* 186 (1999) 255.
- [13] L.D. Mansker, Y. Jin, D.B. Bukur, A.K. Datye, *Appl. Catal. A* 186 (1999) 277.
- [14] M.D. Shroff, D.S. Kalakkad, K.E. Coulter, S.D. Kohler, M.S. Harrington, N.B. Jackson, A.G. Sault, A.K. Datye, *J. Catal.* 156 (1995) 185.
- [15] R. Zhao, J.G. Goodwin Jr., R. Oukaci, *Appl. Catal. A* 189 (1999) 99.
- [16] R. Zhao, J.G. Goodwin Jr., K. Jothimurugesan, J.J. Spivey, S.K. Gangwal, *Ind. Eng. Chem. Res.* 39 (2000) 1155.
- [17] N.B. Jackson, A.K. Datye, L.D. Mansker, R.J. O'Brien, B.H. Davis, in: C.H. Bartholomew, G.A. Fuente (Eds.), *Catalyst Deactivation 1997, Studies in Surface Science and Catalysis*, Vol. 111, Elsevier, New York, 1997, p. 501.
- [18] D.B. Bukur, K. Okabe, M.P. Rosynek, C. Li, D. Wang, K.R.P.M. Rao, G.P. Huffman, *J. Catal.* 155 (1995) 353.
- [19] L.D. Mansker, Y. Jin, D.B. Bukur, A.K. Datye, *Appl. Catal. A* 186 (1999) 277.